Available at
www.ElsevierComputerScience.com
POWERED BY SCIENCE DIRECT®

Signal Processing 85 (2005) 1189–1210

SIGNAL PROCESSING

www.elsevier.com/locate/sigpro

Accuracy of fused track for radar systems

A. Farina[a,*], A. Di Lallo[b], T. Volpi[b], A. Capponi[c,1]

[a]*Chief Technical Office, Alenia Marconi Systems (AMS), Via Tiburtina, Km 12.4, 00131 Rome, Italy*
[b]*Radar & Technology Division, Alenia Marconi Systems (AMS), Via Tiburtina, km 12.4, 00131 Rome, Italy*
[c]*Faculty of Mathematical Sciences, University of Twente, P.O. Box 217, 7500 AE Enschede, The Netherlands*

Received 10 June 2004

Abstract

This paper provides some new results on track fusion for radars. In particular, it provides a relationship between the accuracies of fused tracks for co-located and non co-located radar sensors. The uncertainty volume corresponding to the fused estimate is smaller than the volume of the intersection of the uncertainty ellipsoids associated to the individual sensors. In terms of uncertainty volume, non co-located radars perform better than co-located radars. Analytical results for a study case are reported.

Keywords: Radar; Track fusion; Cramer–Rao lower bound; Uncertainty ellipsoid

1. Introduction

Track-to-track fusion has been the subject of a wide research [1–7]. It has also relevant practical applications for instance in air traffic control systems. One early implementation was for the flight information region of Mazatlan in western Mexico (see [1, pp. 248–254]). The explicit expression of fusion depends on the assumptions concerning the source tracks: they may be either dependent or independent. Two tracks are dependent if the underlined target model has the same process noise (which specifies the target acceleration characteristics) and/or if the a priori knowledge on the target track is shared by the two trackers. The fusion in the dependent tracks case is discussed in [5–8]. A state vector fusion algorithm, which combines the local estimates from each sensor, by taking into account their mutual dependency, was derived in [8]. For track fusion as well as track association, it was recognized in [6] that a non-deterministic

*Corresponding author. Tel.: +39 06 4150 2279; fax: +39 06 4150 2665.
E-mail addresses: afarina@amsjv.it (A. Farina), adilallo@amsjv.it (A. Di Lallo), tvolpi@amsjv.it (T. Volpi), acapponi@cs.caltech.edu (A. Capponi).
[1]Present address: California Institute of Technology, Computer Science, 1200 E. California Blvd, MC 256-80, Pasadena, CA 911525, USA.

0165-1684/$ - see front matter © 2005 Elsevier B.V. All rights reserved.
doi:10.1016/j.sigpro.2004.12.011

target model induces cross-correlation between state estimation errors of local tracks originating from the same target. The performance of track-to-track fusion was evaluated in [5], showing that, as the number of sensors increases, the performance of distributed tracking keeps degrading in comparison with the centralized one. In [7] representative track fusion algorithms and track association metrics were quantitatively compared, varying the non-deterministic components of the target dynamics (i.e. process noises), and the degree of the initial condition uncertainty.

In the present paper we find an analytical relationship regarding the accuracy of the fused track for co-located and non co-located sensors cases. In particular, we developed the theory for a parametric estimation problem rather than for a dynamic state equation problem, showing that, in contrast to the common belief, the uncertainty volume corresponding to the fused estimate is smaller than the volume of the intersection of the uncertainty ellipsoids associated to the individual sensors.

The paper is organized as follows:

- to frame the problem at hand, Section 2 briefly recalls known results concerning the theory of track-to-track fusion;
- Section 3 provides the new results concerning track fusion. It applies the theory to a study case in which the target model is assumed to be a straight line with uniform speed; on the basis of radar measurements, we are interested in estimating the initial position and the speed components of the target and using this estimate to extrapolate the target position ahead in time.
- Section 4 summarizes the main findings of the paper, while Appendices A–C contain mathematical details concerning the most significant results.

2. A review of track fusion

The need for a hierarchical distributed estimation arises when signals are generated by geographically dispersed sensors with limited or costly communications. The steps which must be taken for the estimation of a steady parameter, say $\mathbf{s}$ (e.g. coordinates of initial position, speed components and acceleration of a target) by means of data fusion are depicted in Fig. 1.

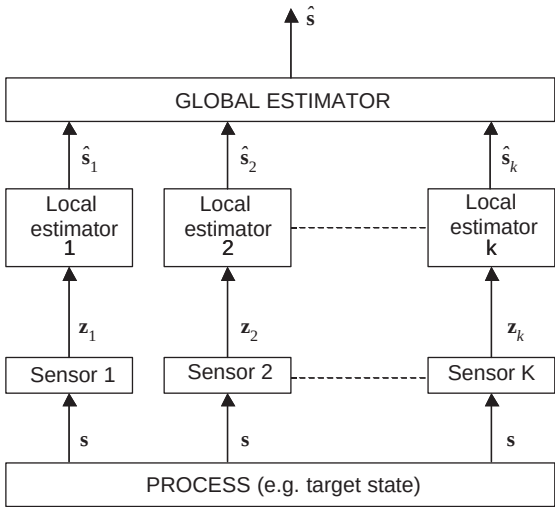

Fig. 1. Hierarchical distributed estimation.

Local estimates are first produced on the purpose of robustness and data compression, then a global estimator combines estimates from local processors to obtain a more accurate estimate of the state. Measurement $\mathbf{z}_i$ (which is available to the generic processor i, with $i = 1, 2, \ldots, k$) is a random variable related to the state. The value of the ith local estimate $\hat{\mathbf{s}}_i$ and the value $\hat{\mathbf{s}}$ of the global estimate of the state are

$$\hat{\mathbf{s}}_i = \mathrm{E}\{\mathbf{s}/\mathbf{z}_i\},$$

$$\hat{\mathbf{s}} = \mathrm{E}\{\mathbf{s}/\mathbf{z}_1, \mathbf{z}_2, \ldots, \mathbf{z}_k\}. \tag{2.1}$$

In the linear and Gaussian case, the local and global estimates are characterized by their mean values $\hat{\mathbf{s}}_i$ and $\hat{\mathbf{s}}$ and by their covariance matrices $\mathbf{P}_i$ and $\mathbf{P}$, respectively.

In the general case of dynamical systems, the rule for data fusion should take account of the time evolution of the state (e.g. the kinematical coordinates of a moving target) and of the possibility of statistical dependence between target tracks [2,8]. Such correlation between tracks generated by different sensors may arise as a consequence of the process noise $w(t)$ affecting the target model. Moreover, local processors estimating the target state may make use of the same initial condition $\mathbf{s}(0)$, with normal distribution $N(\bar{\mathbf{s}}_0, \mathbf{P}_0)$, thus generating additional common information. Whatever the source, statistical dependence between tracks has to be considered and appropriately managed.

Anyway, in the remainder of the paper, independence between tracks will be assumed, justifying the use of the following track fusion algorithm in case of two distinct sensors [1]:

$$\mathbf{P}_f = [\mathbf{P}_1^{-1} + \mathbf{P}_2^{-1}]^{-1},$$

$$\hat{\mathbf{s}}_f = \mathbf{P}_f[\mathbf{P}_1^{-1}\hat{\mathbf{s}}_1 + \mathbf{P}_2^{-1}\hat{\mathbf{s}}_2]. \tag{2.2}$$

The previous equations are easily extended to the case of more than two sensors.

No dynamical equations will be given for the system under consideration, so excluding the common process noise that would otherwise correlate both estimation errors; in fact, we are interested in estimating a steady vector $\mathbf{s}$. Moreover, the unknown state parameter $\mathbf{s}$ will be calculated via the maximum likelihood estimate (MLE) technique, with no a priori information. In conclusion, no common information source will be considered.

3. New results on track fusion

To derive the new results, in Section 3.1 we consider a practical problem, concerning the estimation of a vector of unknown parameters. The fusion of parametric estimates is then discussed in Section 3.2. Having set the scene, the main results of the paper are presented in Section 3.3.

3.1. Study case

Let the trajectory of the target be described by the following equations:[1]

$$x(t) = x_0 + v_x t,$$

$$y(t) = y_0 + v_y t,$$

$$z(t) = z_0 + v_z t, \tag{3.1}$$

[1]A more complex model of target motion could be studied; for instance, the ballistic flight of a missile or of an artillery shell.

where (x_0, y_0, z_0) are the Cartesian coordinates of the target at time t_0 and (v_x, v_y, v_z) are the Cartesian components of the speed. Let $\mathbf{z}_k$ be the kth measurement, out of N, produced by a radar which is the three-dimensional vector as follows:

$$\mathbf{z}_k = \begin{bmatrix} \rho(k) \\ \phi(k) \\ \vartheta(k) \end{bmatrix} = \begin{bmatrix} \sqrt{x(k)^2 + y(k)^2 + z(k)^2} \\ \arcsin \dfrac{z(k)}{\sqrt{x(k)^2 + y(k)^2 + z(k)^2}} \\ \operatorname{arctg} \dfrac{x(k)}{y(k)} \end{bmatrix}$$

$$= \begin{bmatrix} h(\mathbf{s}) \\ f(\mathbf{s}) \\ l(\mathbf{s}) \end{bmatrix} + \mathbf{w}_k \quad k = 1, 2, \ldots, N, \tag{3.2}$$

being $h(\mathbf{s})$, $f(\mathbf{s})$ and $l(\mathbf{s})$ functions of the state $\mathbf{s}$; being $\mathbf{w}_k$ a white Gaussian random variable with zero mean and covariance matrix $\mathbf{R}$

$$\mathbf{R} = \begin{bmatrix} \sigma_\rho^2 & 0 & 0 \\ 0 & \sigma_\phi^2 & 0 \\ 0 & 0 & \sigma_\vartheta^2 \end{bmatrix}, \tag{3.3}$$

where σ_ρ^2, σ_ϕ^2, σ_ϑ^2 are the variances of the three components of the radar measurement; it has been assumed that the three measurements are pairwise independent. The time interval between contiguous radar measurements is T [s].

The goal is to estimate the state vector $\mathbf{s} = [x_0, y_0, z_0, v_x, v_y, v_z]^{\mathrm{T}}$ and use the estimated parameters to predict the target position ahead of the measurement interval. The components of the state vector $\mathbf{s}$ are calculated using the MLE technique as follows [9]:

$$L(\mathbf{s}) = p(\mathbf{z}_1, \mathbf{z}_2, \ldots, \mathbf{z}_N; \mathbf{s})$$
$$= \prod_{k=1}^{N} \frac{1}{\sigma_\rho \sqrt{2\pi}} \exp\left(-\frac{[\rho(k) - h(\mathbf{s}, k)]^2}{2\sigma_\rho^2} \right) \prod_{k=1}^{N} \frac{1}{\sigma_\phi \sqrt{2\pi}} \exp\left(-\frac{[\phi(k) - f(\mathbf{s}, k)]^2}{2\sigma_\phi^2} \right)$$
$$\times \prod_{k=1}^{N} \frac{1}{\sigma_\vartheta \sqrt{2\pi}} \exp\left(-\frac{[\vartheta(k) - l(\mathbf{s}, k)]^2}{2\sigma_\vartheta^2} \right), \tag{3.4}$$

where

$$h(\mathbf{s}, k) = \sqrt{(x_0 + v_x kT)^2 + (y_0 + v_y kT)^2 + (z_0 + v_z kT)^2},$$

$$f(\mathbf{s}, k) = \arcsin \frac{z_0 + v_z kT}{\sqrt{(x_0 + v_x kT)^2 + (y_0 + v_y kT)^2 + (z_0 + v_z kT)^2}},$$

$$l(\mathbf{s}, k) = \operatorname{arctg} \frac{x_0 + v_x kT}{y_0 + v_y kT}, \tag{3.5}$$

with T the time interval between contiguous measurements.

The best estimate of the state vector $\mathbf{s}$ is the state $\hat{\mathbf{s}}$ obtained solving the following maximization problem:

$$\begin{aligned}\hat{\mathbf{s}} &= \arg\max_{\mathbf{s}} p(\mathbf{z}_1, \mathbf{z}_2, \ldots, \mathbf{z}_N; \mathbf{s}) \\ &= \arg\max_{\mathbf{s}} L(\mathbf{s}) = \arg\max_{\mathbf{s}} \ln L(\mathbf{s}).\end{aligned} \tag{3.6}$$

Setting $\lambda(\mathbf{s}) = -\ln L(\mathbf{s})$ and using expression (3.4) for $L(\mathbf{s})$, we obtain after some calculations

$$\lambda(\mathbf{s}) = N[\ln(\sigma_\rho\sqrt{2\pi}) + \ln(\sigma_\phi\sqrt{2\pi}) + \ln(\sigma_\vartheta\sqrt{2\pi})] + \sum_{k=1}^{N}\left\{\frac{[\rho(\mathrm{k}) - h(\mathbf{s},k)]^2}{2\sigma_\rho^2} + \frac{[\phi(\mathrm{k}) - f(\mathbf{s},k)]^2}{2\sigma_\phi^2} + \frac{[\vartheta(\mathrm{k}) - l(\mathbf{s},k)]^2}{2\sigma_\vartheta^2}\right\}. \tag{3.7}$$

The maximization problem (3.6) is equivalent to the following minimization problem

$$\hat{\mathbf{s}} = \arg\min_{\mathbf{s}} \lambda(\mathbf{s}). \tag{3.8}$$

The covariance matrix of the unbiased estimator $\hat{\mathbf{s}}$ is bounded from below by the inverse of the Fisher information matrix (FIM) $\mathbf{J}$ as follows [9]:

$$E\{(\hat{\mathbf{s}} - \mathbf{s})(\hat{\mathbf{s}} - \mathbf{s})^{\mathrm{T}}\} \geqslant \mathbf{J}^{-1}(\hat{\mathbf{s}}),$$

$$\mathbf{J}(\mathbf{s}) = E\{[\nabla_{\mathbf{s}}\lambda(\mathbf{s})][\nabla_{\mathbf{s}}\lambda(\mathbf{s})]^{\mathrm{T}}\}. \tag{3.9}$$

The mathematical expression of the gradient vector $\nabla_{\mathbf{s}}\lambda(\mathbf{s})$ is

$$\begin{aligned}\nabla_{\mathbf{s}}\lambda(\mathbf{s}) &= \nabla_{\mathbf{s}}\frac{1}{2\sigma_\rho^2}\sum_{k=1}^{N}[\rho(k) - h(\mathbf{s},k)]^2 + \nabla_{\mathbf{s}}\frac{1}{2\sigma_\phi^2}\sum_{k=1}^{N}[\phi(k) - f(\mathbf{s},k)]^2 \\ &\quad + \nabla_{\mathbf{s}}\frac{1}{2\sigma_\vartheta^2}\sum_{k=1}^{N}[\vartheta(k) - l(\mathbf{s},k)]^2 \\ &= \frac{1}{2\sigma_\rho^2}\sum_{k=1}^{N}\nabla_{\mathbf{s}}[\rho(k) - h(\mathbf{s},k)]^2 + \frac{1}{2\sigma_\phi^2}\sum_{k=1}^{N}\nabla_{\mathbf{s}}[\phi(k) - f(\mathbf{s},k)]^2 \\ &\quad + \frac{1}{2\sigma_\vartheta^2}\sum_{k=1}^{N}\nabla_{\mathbf{s}}[\vartheta(k) - l(\mathbf{s},k)]^2 \\ &= -\frac{1}{\sigma_\rho^2}\sum_{k=1}^{N}[\rho(k) - h(\mathbf{s},k)]\nabla_{\mathbf{s}}h(\mathbf{s},k) - \frac{1}{\sigma_\phi^2}\sum_{k=1}^{N}[\phi(k) - f(\mathbf{s},k)]\nabla_{\mathbf{s}}f(\mathbf{s},k) \\ &\quad - \frac{1}{\sigma_\vartheta^2}\sum_{k=1}^{N}[\vartheta(k) - l(\mathbf{s},k)]\nabla_{\mathbf{s}}l(\mathbf{s},k).\end{aligned} \tag{3.10}$$

Under the assumptions that the three components of the radar measurements are pair wise independent we have

$$\begin{aligned}\mathbf{J} &= \frac{1}{\sigma_\rho^4}\sum_{k=1}^{N} E\{[\rho(k)-h(\mathbf{s},k)]^2\}\nabla_{\mathbf{s}}h(\mathbf{s},k)(\nabla_{\mathbf{s}}h(\mathbf{s},k))^{\mathrm{T}} \\ &\quad + \frac{1}{\sigma_\phi^4}\sum_{k=1}^{N} E\{[\phi(k)-f(\mathbf{s},k)]^2\}\nabla_{\mathbf{s}}f(\mathbf{s},k)(\nabla_{\mathbf{s}}f(\mathbf{s},k))^{\mathrm{T}} \\ &\quad + \frac{1}{\sigma_\vartheta^4}\sum_{k=1}^{N} E\{[\vartheta(k)-l(\mathbf{s},k)]^2\}\nabla_{\mathbf{s}}l(\mathbf{s},k)(\nabla_{\mathbf{s}}l(\mathbf{s},k))^{\mathrm{T}} \\ &= \sum_{k=1}^{N}\left\{\frac{1}{\sigma_\rho^2}\nabla_{\mathbf{s}}h(\mathbf{s},k)(\nabla_{\mathbf{s}}h(\mathbf{s},k))^{\mathrm{T}} + \frac{1}{\sigma_\phi^2}\nabla_{\mathbf{s}}f(\mathbf{s},k)(\nabla_{\mathbf{s}}f(\mathbf{s},k))^{\mathrm{T}} + \frac{1}{\sigma_\vartheta^2}\nabla_{\mathbf{s}}l(\mathbf{s},k)(\nabla_{\mathbf{s}}l(\mathbf{s},k))^{\mathrm{T}}\right\}. \end{aligned} \tag{3.11}$$

The gradient vectors $\nabla_{\mathbf{s}}h(\mathbf{s},k)$, $\nabla_{\mathbf{s}}f(\mathbf{s},k)$ and $\nabla_{\mathbf{s}}l(\mathbf{s},k)$ have the following components:

$$\nabla_{\mathbf{s}}h(\mathbf{s},k) = \begin{cases} [\nabla_{\mathbf{s}}h(\mathbf{s},k)]_{x_0} = \dfrac{x[k]}{\sqrt{(x[k])^2+(y[k])^2+(z[k])^2}}, \\ [\nabla_{\mathbf{s}}h(\mathbf{s},k)]_{y_0} = \dfrac{y[k]}{\sqrt{(x[k])^2+(y[k])^2+(z[k])^2}}, \\ [\nabla_{\mathbf{s}}h(\mathbf{s},k)]_{z_0} = \dfrac{z[k]}{\sqrt{(x[k])^2+(y[k])^2+(z[k])^2}}, \\ [\nabla_{\mathbf{s}}h(\mathbf{s},k)]_{v_x} = kT\,[\nabla_{\mathbf{s}}h(\mathbf{s},k)]_{x_0}, \\ [\nabla_{\mathbf{s}}h(\mathbf{s},k)]_{v_y} = kT\,[\nabla_{\mathbf{s}}h(\mathbf{s},k)]_{y_0}, \\ [\nabla_{\mathbf{s}}h(\mathbf{s},k)]_{v_z} = kT\,[\nabla_{\mathbf{s}}h(\mathbf{s},k)]_{z_0}, \end{cases} \tag{3.12}$$

$$\nabla_{\mathbf{s}}f(\mathbf{s},k) = \begin{cases} [\nabla_{s}f(\mathbf{s},k)]_{x_0} \\ \quad = \dfrac{-x[k]\,z[k]}{[(x[k])^2+(y[k])^2+(z[k])^2]\sqrt{(x[k])^2+(y[k])^2}}, \\ [\nabla_{\mathbf{s}}f(\mathbf{s},k)]_{y_0} \\ \quad = \dfrac{-y[k]\,z[k]}{[(x[k])^2+(y[k])^2+(z[k])^2]\sqrt{(x[k])^2+(y[k])^2}}, \\ [\nabla_{\mathbf{s}}f(\mathbf{s},k)]_{z_0} = \dfrac{\sqrt{(x[k])^2+(y[k])^2}}{[(x[k])^2+(y[k])^2+(z[k])^2]}, \\ [\nabla_{\mathbf{s}}f(\mathbf{s},k)]_{v_x} = kT\,[\nabla_{\mathbf{s}}f(\mathbf{s},k)]_{x_0}, \\ [\nabla_{\mathbf{s}}f(\mathbf{s},k)]_{v_y} = kT\,[\nabla_{\mathbf{s}}f(\mathbf{s},k)]_{y_0}, \\ [\nabla_{\mathbf{s}}f(\mathbf{s},k)]_{v_z} = kT\,[\nabla_{\mathbf{s}}f(\mathbf{s},k)]_{z_0}, \end{cases} \tag{3.13}$$

$$\nabla_{\mathbf{s}} l(\mathbf{s},k)=\begin{cases}[\nabla_{\mathbf{s}} l(\mathbf{s},k)]_{x_0}=\dfrac{y[k]}{[(x[k])^2+(y[k])^2]},\\ [\nabla_{\mathbf{s}} l(\mathbf{s},k)]_{y_0}=-\dfrac{x[k]}{[(x[k])^2+(y[k])^2]},\\ [\nabla_{\mathbf{s}} l(\mathbf{s},k)]_{z_0}=0,\\ [\nabla_{\mathbf{s}} l(\mathbf{s},k)]_{v_x}=kT\,[\nabla_{\mathbf{s}} l(\mathbf{s},k)]_{x_0},\\ [\nabla_{\mathbf{s}} l(\mathbf{s},k)]_{v_y}=kT\,[\nabla_{\mathbf{s}} l(\mathbf{s},k)]_{y_0},\\ [\nabla_{\mathbf{s}} l(\mathbf{s},k)]_{v_z}=0,\end{cases} \tag{3.14}$$

where $x[k]$, $y[k]$ and $z[k]$ denote the ideal position along the three Cartesian coordinates of the target in the kth time instant.

The evaluation of expressions (3.12, 3.13, 3.14) finally enables us to calculate the FIM (3.11). After inversion of matrix $\mathbf{J}$, the Cramer–Rao lower bound (CRLB) for the estimated vector $\mathbf{s}$ of target parameters (i.e. the covariance matrix of the unbiased estimator $\hat{\mathbf{s}}$) is obtained

$$\mathbf{CRLB}=\begin{bmatrix}\sigma_{x_0}^2 & \sigma_{x_0y_0} & \sigma_{x_0z_0} & \sigma_{x_0v_x} & \sigma_{x_0v_y} & \sigma_{x_0v_z}\\ \sigma_{x_0y_0} & \sigma_{y_0}^2 & \sigma_{y_0z_0} & \sigma_{y_0v_x} & \sigma_{y_0v_y} & \sigma_{y_0v_z}\\ \sigma_{x_0z_0} & \sigma_{y_0z_0} & \sigma_{z_0}^2 & \sigma_{z_0v_x} & \sigma_{z_0v_y} & \sigma_{z_0v_z}\\ \sigma_{x_0v_x} & \sigma_{y_0v_x} & \sigma_{z_0v_x} & \sigma_{v_x}^2 & \sigma_{v_xv_y} & \sigma_{v_xv_z}\\ \sigma_{x_0v_y} & \sigma_{y_0v_y} & \sigma_{z_0v_y} & \sigma_{v_xv_y} & \sigma_{v_y}^2 & \sigma_{v_yv_z}\\ \sigma_{x_0v_z} & \sigma_{y_0v_z} & \sigma_{z_0v_z} & \sigma_{v_xv_z} & \sigma_{v_yv_z} & \sigma_{v_z}^2\end{bmatrix}. \tag{3.15}$$

Assume now that we wish to predict the target state ahead in time after the acquisition of N radar measurements; we are interested in the target position in kT instants with $k>N$. We achieve the purpose by inserting the target state vector $\hat{\mathbf{s}}$, estimated by the N radar measurements, in the target model (3.1) which will be calculated at the kth time instant. The corresponding covariance matrix $\mathbf{P}$ of the predicted target position is

$$\mathbf{P}=\begin{bmatrix}\sigma_x^2 & \sigma_{xy} & \sigma_{xz}\\ \sigma_{xy} & \sigma_y^2 & \sigma_{yz}\\ \sigma_{xz} & \sigma_{yz} & \sigma_z^2\end{bmatrix}, \tag{3.16}$$

where

$$\sigma_x^2(kT)=\sigma_{x_0}^2+\sigma_{v_x}^2\,(kT)^2+2\sigma_{x_0v_x}\,(kT),$$

$$\sigma_y^2(kT)=\sigma_{y_0}^2+\sigma_{v_y}^2\,(kT)^2+2\sigma_{y_0v_y}\,(kT),$$

$$\sigma_z^2(kT)=\sigma_{z_0}^2+\sigma_{v_z}^2\,(kT)^2+2\sigma_{z_0v_z}\,(kT),$$

$$\sigma_{xy}(kT)=\sigma_{x_0y_0}+(\sigma_{y_0v_x}+\sigma_{x_0v_y})\,(kT)+\sigma_{v_xv_y}\,(kT)^2,$$

$$\sigma_{xz}(kT)=\sigma_{x_0z_0}+(\sigma_{z_0v_x}+\sigma_{x_0v_z})\,(kT)+\sigma_{v_xv_z}\,(kT)^2,$$

$$\sigma_{yz}(kT)=\sigma_{y_0z_0}+(\sigma_{y_0v_z}+\sigma_{z_0v_y})\,(kT)+\sigma_{v_yv_z}\,(kT)^2.$$

The variances and co-variances in the equation above are given by the **CRLB** (3.15).

3.2. Fusion of estimates

When two or more sensors are present, the combination of their actions gives rise to a multi-sensor configuration. In this case, we consider two radars which are tracking the same target and processing the measured data, as depicted in Fig. 2.

The use of the distributed architecture [1] aims at improving the accuracy of the prediction of target trajectory. To this purpose, we need to calculate the covariance matrix of the target extrapolated position, after that each radar has collected the N independent measurements.

The steps to take are:

1. evaluation of $\mathbf{CRLB}_1$ associated to the target state as perceived from radar 1;
2. evaluation of $\mathbf{CRLB}_2$ associated to the target state as perceived from radar 2;
3. evaluation of $\mathbf{CRLB}_f$ for the estimated vector $\hat{\mathbf{s}}_f$ obtained after the track fusion by combination of the *CRLB* matrices of each estimated vector [1,2]:

$$\mathbf{CRLB}_f = (\mathbf{CRLB}_1^{-1} + \mathbf{CRLB}_2^{-1})^{-1} \tag{3.17}$$

4. calculation of the covariance matrix $\mathbf{P}_f$ of the extrapolated trajectory from $\mathbf{CRLB}_f$ according to (3.16).

We note that the previous fusion equation (3.17) holds true only when the tracks are independent, which is our case; when the tracks are dependent random variables, a modified equation should be applied, as specified in [8].

The following numerical experiment has been conducted. There are two radar sensors S_1 and S_2 which are located, respectively, at the coordinates $(0,0,0)$ and $(-10,-10,0)$. Each coordinate is expressed in [km]. The position of the radar sensor S_1 is in center of the Cartesian reference system. The standard deviations of the three components of the radar measurements are assumed to be the same for both radars.

The standard deviation in range is set to 100 [m], while the standard deviations in azimuth and elevation are both set to 0.2°. The data rate T is set to 12 [s], the number N of measurements used by both radars for the estimation is set to 10, the target tracks are predicted at instant $5T$ after the last processed plot. In Fig. 3 we note that the 3rd plot of the ideal trajectory of the target is the 1st plot used for the estimation of the state vector $\mathbf{s}$. The true value of the initial target position vector, expressed in [km], is $(x_0, y_0, z_0) = (10, 10, 10)$, while the target velocity vector, expressed in [m/s], is $(v_x, v_y, v_z) = (100, 100, 100)$.

Under the assumptions described above, the uncertainty ellipsoids associated to the target tracks predicted by the radar sensors S_1 and S_2, and the uncertainty ellipsoid associated to the target track resulting from the fusion of the two covariance matrices $\mathbf{CRLB}_1$ and $\mathbf{CRLB}_2$, appear as shown in Fig. 3.

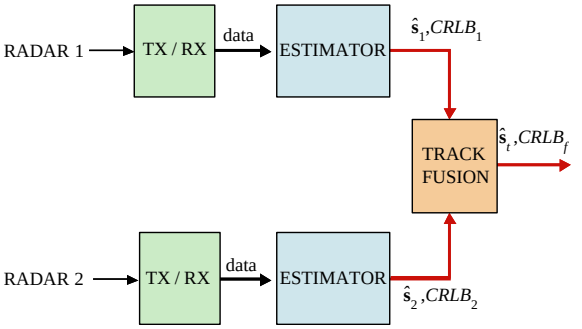

Fig. 2. Distributed architecture for track fusion and CRLB evaluation.

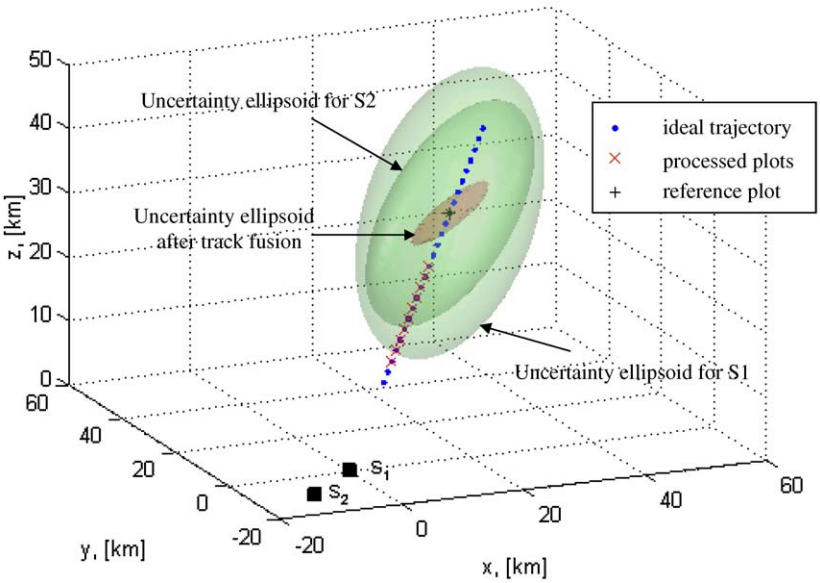

Fig. 3. Uncertainty ellipsoids associated to the target tracks estimated by sensors S_1 and S_2 and to their fusion; the reference plot is the one to which the uncertainty ellipsoids are referred to.

The equation of each ellipsoid is

$$\{\mathbf{s}^{\mathrm{T}}\mathbf{P}_i^{-1}\mathbf{s} \leqslant r^2\}, \quad i = 1, 2, f, \tag{3.18}$$

where $\mathbf{P}_1$ and $\mathbf{P}_2$ denote the covariance matrices of the extrapolated trajectory calculated using $\mathbf{CRLB}_1$ and $\mathbf{CRLB}_2$, respectively, while $\mathbf{P}_f$ is the covariance matrix of the extrapolated trajectory calculated using $\mathbf{CRLB}_f$.

The value r is set to 3, which gives a 99% probability that the unknown target position falls within the ellipsoid.

3.3. Main results

In Fig. 3 the ideal target trajectory is represented by a sequence of plots (•), occurring every T seconds: N plots (×) are processed to evaluate the state vector $\mathbf{s}$ covariance matrices, one plot (+) is chosen to show the uncertainty ellipsoids for the extrapolated trajectory. We note that the uncertainty ellipsoid of the fused track is much smaller than the intersection of the ellipsoids relative to tracks 1 and 2. This is in contrast to the common belief that the accuracy of the fused track is related just to the intersection of the individual tracks accuracies. To be more precise, we state the following results concerning the volumes of the uncertainty ellipsoids taken as a suitable measurement of the track accuracy.

The volume of the uncertainty ellipsoid of the fused track is related to the volumes of the uncertainty ellipsoids of individual tracks by the following equation:

$$V_f = r^n c(n) \frac{1}{\sqrt{\det(\mathbf{P}_f^{-1})}}, \tag{3.19}$$

where $\mathbf{P}_f^{-1} = \mathbf{P}_1^{-1} + \mathbf{P}_2^{-1}$. The value r is such that the probability of the random variable $\{s^{\mathrm{T}}\mathbf{P}_i^{-1}\mathbf{s}\}$ is not greater than r^2 and $c(n)$ is the volume of the unit hypersphere.

The volume V_f is not greater than the volume $V_{\parallel}$

$$V_{\parallel} = \frac{V_1 V_2}{V_1 + V_2}, \tag{3.20}$$

that would be obtained applying the so-called rule of "parallel resistances" to the volumes V_1 and V_2 of the uncertainty ellipsoids of tracks 1 and 2. The proof of this statement is given in Appendix A.

In Appendix B we further develop this result referring to a target on the x–y plane. In particular, we find results for the co-located and non co-located sensors cases. For the co-located case we find

$$A_f = \frac{A}{2}. \tag{3.21}$$

Eq. (3.21) shows that the uncertainty area A_f associated to the fused track halves with respect to the uncertainty area A relative to each individual track (sensors are co-located and identical to each other). A physical explanation is also given. For the non co-located case we have

$$A_f \leqslant \frac{A_1 A_2}{A_1 + A_2}. \tag{3.22}$$

Eq. (3.22) states that the target parameter estimate obtained using two separate radars and fusing their tracks is more accurate than the estimate that would be obtained by applying the rule for "parallel resistances" ($A_f \leqslant A_{\parallel}$). The equality holds (i.e. $A_f = A_{\parallel}$) in two particular cases:

- the radars are co-located;
- the covariance matrices of the local estimates can be respectively expressed as $\mathbf{P}_1 = \sigma_1^2 \cdot \mathbf{I}$ and $\mathbf{P}_2 = \sigma_2^2 \cdot \mathbf{I}$, where $\mathbf{I}$ is the identity matrix.

Finally, in Appendix 3 we extend the previous results to $k > 2$ sensors, showing again that $V_f \leqslant V_{\parallel}$.

In summary, the upper bound to V_f is given by the so-called rule of "parallel resistances". Concerning the lower bound to V_f, the following considerations are in order.

For the sake of simplicity, the analysis is limited to the 2D case. Two sensors S_1 and S_2, characterized by the same values of measurement accuracies ($\sigma_\rho = 50\,\mathrm{m},\ \sigma_\theta = 0.2^\circ$), are respectively located in $(-10, 0)$ and $(10, 0)$, being the coordinates expresses in km.

The target position is assumed to vary in the x–y plane defined by the interval $(-20, 20)$ km for the x-coordinate and $(-20, 20)$ km for the y-coordinate. The area of the uncertainty ellipse resulting from track fusion for each target position is depicted in Fig. 4. Note that the plot is symmetrical with respect to the horizontal line S_1–S_2. The contour plot represents the uncertainty area, normalized to its maximum value, in dB units. The minimum value of the uncertainty area is obtained when the target position is $(0, 10)$ km, i.e. when the lines of sight sensor-target are perpendicular to each other. In this configuration, in fact, the major axis of the S_1 individual uncertainty ellipse is combined with the minor axis of the S_2 individual uncertainty ellipse, and vice versa. The consequent minimization of the result of track fusion can be justified reminding the relationship $\rho\,\sigma_\vartheta > \sigma_\rho$, which generally holds for radars. If the two individual ellipses are perpendicular to each other (i.e. the major axis of S_1 is perpendicular to the minor axis of S_2 and vice versa) and their minor axes are both equal to σ_ρ, the area of the uncertainty ellipse resulting from track fusion cannot be greater than the "safe area" $\pi\,\sigma_\rho^2$. A geometrical explanation for the lower bound to track fusion in the 2D case is shown in Fig. 5. If the radars have different range accuracies, the area of the fused ellipse is less than $\pi\,\sigma_{\rho,1}\,\sigma_{\rho,2}$.

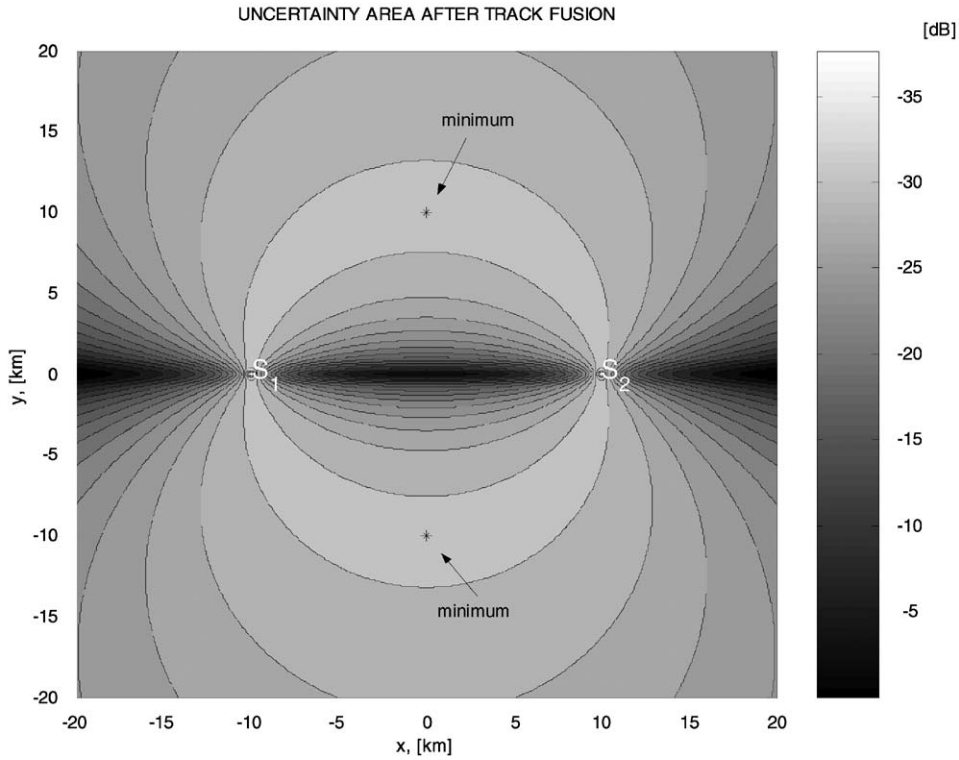

Fig. 4. Cantour plot of the uncertainty area resulting from track fusion for varying target position. The area is normalized to its maximum value and expressed in dB units.

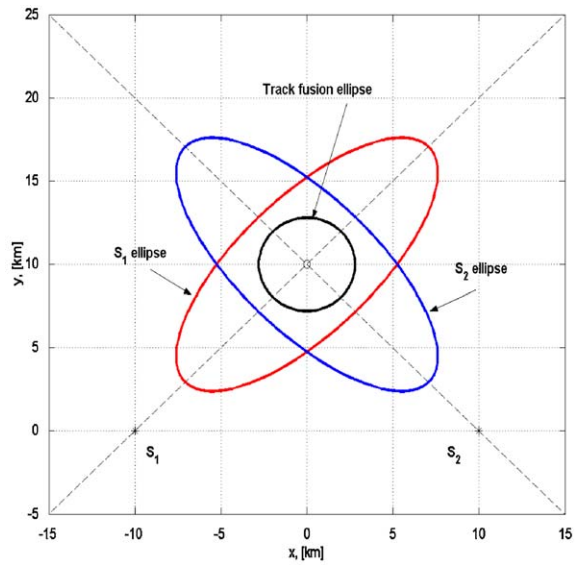

Fig. 5. The lower limit to track fusion in the 2D case.

3.3.1. Fusion gain with respect to individual radars

It is assumed that the radar sensors are *co-located* and the signal to noise ratio (SNR) is the same for each sensor. The following equalities apply:

$$1D \Leftrightarrow \sigma_f = \frac{1}{\sqrt{2}}\sigma,$$

$$2D \Leftrightarrow A_f = \tfrac{1}{2}A,$$

$$3D \Leftrightarrow V_f = \frac{1}{2\sqrt{2}}V. \tag{3.23}$$

The result relative to the $1D$ case directly follows from the expression for the theoretical error ΔM of a radar measurement M [10]:

$$\Delta M = \frac{kM}{\sqrt{2\mathrm{SNR}}}, \tag{3.24}$$

where the parameters k and M depend on the extracted measurement which can be either range, bearing or elevation. In the fused case, the SNR value doubles because either the transmitted power or the radiated number of pulses double.

For 2D radars the track resulting from the fusion of two tracks coming from two different radars provides an accuracy that is better than the accuracy of each single track of a factor equal to $\frac{1}{2}$: see (B.23) of Appendix B.

In the case of 3D radars, the volume V_f of the ellipsoid of uncertainty associated to the equivalent system consisting of only one radar sensor is $1/2\sqrt{2}$ of the volume of the ellipsoid of uncertainty associated to each of the two radar sensors. Intuitively, this value comes from the product of $1/\sqrt{2}$ reduction factors along each one of the three axes.

In the general case of n-dimensional target state and k *non co-located* radars, the following result has been found. Let $E_1 = \{\mathbf{s}^{\mathrm{T}}\mathbf{P}_1^{-1}\mathbf{s} \leqslant r^2\}$, $E_2 = \{\mathbf{s}^{\mathrm{T}}\mathbf{P}_2^{-1}\mathbf{s} \leqslant r^2\}, \ldots,$ and $E_k = \{\mathbf{s}^{\mathrm{T}}\mathbf{P}_k^{-1}\mathbf{s} \leqslant r^2\}$ be the n dimensional uncertainty ellipsoids associated to k non co-located radars. Let $\mathbf{P}_f^{-1} = \mathbf{P}_1^{-1} + \mathbf{P}_2^{-1} + \cdots + \mathbf{P}_k^{-1}$ and assume without loss of generality that E_1 has the maximum volume denoted by V_1. It can be shown that (see Appendix D for the detailed proof)

$$\frac{V_f}{V_1} \leqslant \frac{1}{k}. \tag{3.25}$$

4. Conclusions

In this paper we have investigated the track-to-track fusion for radar systems, developing the theory for a parametric estimation problem. In particular, we have assumed the independence of the tracks, as a consequence of the absence of a common process noise (which is instead typical of dynamical states) and of any a priori statistical information on the state to estimate.

To derive our results, we have considered a target moving along a straight line in a Cartesian reference system (x, y, z), even though other trajectories can be considered, as, for instance, the ballistic target motion. On the basis of N measurements, we have first evaluated the CRLB matrices associated to each sensor and to their track fusion. We have then calculated the covariance matrices of the extrapolated trajectory ahead in the time interval. The volume of the ellipsoid has been taken as a metric of track quality. We have shown that the prediction accuracy of the target position not only improves by fusing the tracks, but the

improvement factor is larger than the simple intersection of the uncertainty ellipsoids of the individual sensors. Equations for a number of study cases have been provided to measure the fusion gain.

Appendix A

Consider two distinct radar sensors S_1 and S_2. Let $E_1 = \{\mathbf{s}^T\mathbf{P}_1^{-1}\mathbf{s} \leqslant r^2\}$ and $E_2 = \{\mathbf{s}^T\mathbf{P}_2^{-1}\mathbf{s} \leqslant r^2\}$ be the uncertainty ellipsoids associated, respectively, to the target tracks estimated by S_1 and S_2, where $\mathbf{s}$ represents the n-dimensional target state vector and $\mathbf{P}_1$ and $\mathbf{P}_2$ are n by n positive definite matrices representing the covariance matrices of the two tracks. The objective of this appendix is to show that the volume V_f of the equivalent ellipsoid, which gives a measure of the accuracy of the fused track

$$V_f = r^n c(n) \frac{1}{\sqrt{\det(\mathbf{P}_f^{-1})}}, \tag{A.1}$$

where $\mathbf{P}_f^{-1} = \mathbf{P}_1^{-1} + \mathbf{P}_2^{-1}$, is not greater than the volume $V_{\parallel}$ obtained applying the rule of parallel resistances to the volumes V_1 and V_2

$$V_{\parallel} = \frac{V_1 V_2}{V_1 + V_2}, \tag{A.2}$$

where $V_i = r^n c(n) 1/\sqrt{\det(\mathbf{P}_i^{-1})}$ [11], $i = 1, 2$, denotes the volume of the ellipsoid of uncertainty E_i associated to the target track provided by sensor S_i. The value r is such that the probability of the random variable $\{\mathbf{s}^T\mathbf{P}_i^{-1}\mathbf{s}\}$ is not greater than r^2 and $c(n)$ is the volume of the unit hypersphere as follows:

$$c(n) = \frac{\pi^{n/2}}{(n/2)!} \text{ if } n \text{ is even},$$

$$c(n) = \frac{2^n \pi^{n-1/2}(n - 1/2)!}{n!} \text{ if } n \text{ is odd}. \tag{A.3}$$

The proof of this result is based upon the following well known inequality concerning the determinant of the sum of two positive definite matrices. It states:

Lemma 1 ([12]). *Let* $\mathbf{A}_1$ *and* $\mathbf{A}_2$ *be two n-dimensional positive definite matrices,* $n \geqslant 1$. *Then it is true*

$$\sqrt[n]{\det(\mathbf{A}_1 + \mathbf{A}_2)} \geqslant \sqrt[n]{\det(\mathbf{A}_1)} + \sqrt[n]{\det(\mathbf{A}_2)}. \tag{A.4}$$

Applying the lemma above, the following corollary can be proved.

Corollary 2. *Let* $\mathbf{A}_1$ *and* $\mathbf{A}_2$ *be two n-dimensional positive definite matrices,* $n \geqslant 2$. *Set an integer* $m \leqslant n$ *we have*

$$\sqrt[m]{\det(\mathbf{A}_1 + \mathbf{A}_2)} \geqslant \sqrt[m]{\det(\mathbf{A}_1)} + \sqrt[m]{\det(\mathbf{A}_2)}. \tag{A.5}$$

Proof. The proof of the corollary depends on the validity of the following statement.

Statement 3. *For every* $p \geqslant 1$, *a and b positive real numbers we have that*

$$(a + b)^p \geqslant a^p + b^p. \tag{A.6}$$

Proof of Statement 3. Consider the function $f(x) = (x + b)^p - x^p - b^p$. Then $f(0) = 0$ and $\dot{f}(x) \geqslant 0$ for every $x \geqslant 0$ ($\dot{f}$ denotes the first-order derivative of f). All that leads to the conclusion that f is an increasing function which takes the value 0 when $x = 0$. Hence, $f(x) \geqslant 0$ for every $x \geqslant 0$. Substituting the unknown term x with the positive term a, we get that $f(a) = (a + b)^p - a^p - b^p \geqslant 0$, so the inequality has been verified.

Choose $a = \sqrt[n]{\det(\mathbf{A}_1)}$, $b = \sqrt[n]{\det(\mathbf{A}_2)}$ and $p = n/m$. The fact that $\mathbf{A}_1$ and $\mathbf{A}_2$ are both positive definite matrices means that $\det(\mathbf{A}_1)$ and $\det(\mathbf{A}_2)$ are positive values which itself implies that a and b are both positive real numbers. Also note that $m \leqslant n$ by the hypothesis of the corollary, thus $p \geqslant 1$. □

Since a and b are both positive real numbers and $p \geqslant 1$, we have by the inequality (A.6) that

$$\begin{aligned}(\sqrt[n]{\det(\mathbf{A}_1)} + \sqrt[n]{\det(\mathbf{A}_2)})^{n/m} &\geqslant (\sqrt[n]{\det(\mathbf{A}_1)})^{n/m} + (\sqrt[n]{\det(\mathbf{A}_2)})^{n/m} \\ &= \sqrt[m]{\det(\mathbf{A}_1)} + \sqrt[m]{\det(\mathbf{A}_2)}. \end{aligned} \tag{A.7}$$

The application of Lemma 1 leads to the inequality

$$(\sqrt[n]{\det(\mathbf{A}_1) + \det(\mathbf{A}_2)}) \geqslant (\sqrt[n]{\det(\mathbf{A}_1)} + \sqrt[n]{\det(\mathbf{A}_2)}), \tag{A.8}$$

which combined with the increasing of the exponential function gives

$$(\sqrt[n]{\det(\mathbf{A}_1) + \det(\mathbf{A}_2)})^{n/m} \geqslant (\sqrt[n]{\det(\mathbf{A}_1)} + \sqrt[n]{\det(\mathbf{A}_2)})^{n/m}. \tag{A.9}$$

Hence, combining (A.7) and (A.9) we obtain

$$(\sqrt[n]{\det(\mathbf{A}_1) + \det(\mathbf{A}_2)})^{n/m} \geqslant \sqrt[m]{\det(\mathbf{A}_1)} + \sqrt[m]{\det(\mathbf{A}_2)}. \tag{A.10}$$

After the simplification of the first term in the above inequality, it follows that

$$\sqrt[m]{\det(\mathbf{A}_1) + \det(\mathbf{A}_2)} \geqslant \sqrt[m]{\det(\mathbf{A}_1)} + \sqrt[m]{\det(\mathbf{A}_2)}, \tag{A.11}$$

which is exactly the thesis of the Corollary 2. □

At this point there are all the ingredients needed to prove the main result of this appendix which is stated in the form of the following theorem.

Theorem 4. *$V_f \leqslant V_{\|}$, where V_f and $V_{\|}$ have been defined in* (A.1) *and* (A.2) *respectively.*

Proof. After simplifying terms, it follows that $V_f \leqslant V_{\|}$ if and only if

$$r^n c(n) \frac{1}{\sqrt{\det(\mathbf{P}_f^{-1})}} \leqslant r^n c(n) \frac{1}{(\sqrt{\det(\mathbf{P}_1^{-1})} + \sqrt{\det(\mathbf{P}_2^{-1})})}, \tag{A.12}$$

which is true if and only if

$$\sqrt{\det(\mathbf{P}_f^{-1})} \geqslant \sqrt{\det(\mathbf{P}_1^{-1})} + \sqrt{\det(\mathbf{P}_2^{-1})}. \tag{A.13}$$

Since the order of the matrices $\mathbf{P}_1^{-1}$ and $\mathbf{P}_2^{-1}$ is at least 2 the inequality above is guaranteed to be true by Corollary 2. □

Appendix B

In this appendix we consider a simple location problem to further demonstrate the general result of Appendix A. A steady target having location (x, y) is sensed by two non co-located radars S_1 and S_2. In this two-dimensional case (i.e. $n = 2$), the equation defining the uncertainty ellipse associated to the target position and to the generic radar becomes

$$\mathbf{s}^{\mathrm{T}}\mathbf{P}^{-1}\mathbf{s} = [x \;\; y] \begin{bmatrix} \sigma_x^2 & \sigma_{xy} \\ \sigma_{xy} & \sigma_y^2 \end{bmatrix}^{-1} \begin{bmatrix} x \\ y \end{bmatrix} \leqslant r^2. \tag{B.1}$$

The state vector **s** consists of two Gaussian random variables (x, y), with variances σ_x^2 and σ_y^2, respectively, and correlation coefficient $\rho = \sigma_{xy}/\sigma_x\sigma_y$. Eq. (B.1) describes an ellipse E in the arbitrary form $ax^2 + bxy + cy^2 \leqslant r^2$

$$\frac{1}{1-\rho^2}\left[\left(\frac{x}{\sigma_x}\right)^2 + \left(\frac{y}{\sigma_y}\right)^2 - 2\rho\frac{xy}{\sigma_x\sigma_y}\right] \leqslant r^2. \tag{B.2}$$

The uncertainty area A is then given by

$$A = r^2\frac{2\pi}{\sqrt{4ac-b^2}} = r^2\,\pi\sqrt{\sigma_x^2\sigma_y^2 - \sigma_{xy}^2}. \tag{B.3}$$

Two distinct radars S_1 and S_2 generate two different two-dimensional joint Gaussian estimates (x_1, y_1) and (x_2, y_2), with covariance matrices $\mathbf{P}_1$ and $\mathbf{P}_2$ and uncertainty areas A_1 and A_2, respectively. The covariance matrix obtained after the track fusion is

$$\mathbf{P}_f = (\mathbf{P}_1^{-1} + \mathbf{P}_2^{-1})^{-1}. \tag{B.4}$$

Eq. (B.4) can also be expressed in terms of variances and co-variances

$$\begin{bmatrix} \sigma_{x,f}^2 & \sigma_{xy,f} \\ \sigma_{xy,f} & \sigma_{y,f}^2 \end{bmatrix} = \left[\begin{bmatrix} \sigma_{x,1}^2 & \sigma_{xy,1} \\ \sigma_{xy,1} & \sigma_{y,1}^2 \end{bmatrix}^{-1} + \begin{bmatrix} \sigma_{x,2}^2 & \sigma_{xy,2} \\ \sigma_{xy,2} & \sigma_{y,2}^2 \end{bmatrix}^{-1}\right]^{-1}. \tag{B.5}$$

After some computation, we finally obtain

$$\mathbf{P}_f = \frac{1}{A_1^2 + A_2^2 + \pi^2\cdot T_{1,2}} \begin{bmatrix} \sigma_{x,1}^2 A_2^2 + \sigma_{x,2}^2 A_1^2 & \sigma_{xy,1} A_2^2 + \sigma_{xy,2} A_1^2 \\ \sigma_{xy,1} A_2^2 + \sigma_{xy,2} A_1^2 & \sigma_{y,1}^2 A_2^2 + \sigma_{y,2}^2 A_1^2 \end{bmatrix}, \tag{B.6}$$

where $T_{1,2}$ is defined as follows:

$$T_{1,2} = \sigma_{x,1}^2\,\sigma_{y,2}^2 + \sigma_{x,2}^2\,\sigma_{y,1}^2 - 2\,\sigma_{xy,1}\,\sigma_{xy,2}. \tag{B.7}$$

According to Eq. (B.3) and assuming for sake of simplicity $r = 1$, the uncertainty area of the estimate resulting from the fusion of the tracks, respectively, generated by radars S_1 and S_2 is

$$A_f = \pi\sqrt{\sigma_{x,f}^2\,\sigma_{y,f}^2 - \sigma_{xy,f}^2} = \frac{A_1 A_2}{\sqrt{A_1^2 + A_2^2 + \pi^2\,T_{1,2}}}. \tag{B.8}$$

Our goal is to demonstrate that the uncertainty area A_f relative to the track fusion estimate is equal to or smaller than the uncertainty area $A_\parallel$ that would be obtained applying the rule for in parallel resistances

$$A_\parallel = \left(\frac{1}{A_1} + \frac{1}{A_2}\right)^{-1} = \frac{A_1\,A_2}{A_1 + A_2}. \tag{B.9}$$

The aim is to prove that $A_f \leqslant A_\parallel$; according to expressions (B.8) and (B.9), this reduces to prove

$$\frac{A_1\,A_2}{\sqrt{A_1^2 + A_2^2 + \pi^2\,T_{1,2}}} \leqslant \frac{A_1\,A_2}{A_1 + A_2}. \tag{B.10}$$

Since the two numerators are identical, we can limit our analysis to the denominators, which are expected to verify the equation

$$\sqrt{A_1^2 + A_2^2 + \pi^2\,T_{1,2}} \geqslant A_1 + A_2. \tag{B.11}$$

Since A_1 and A_2 are both positive, the second term in Eq. (B.11) can also be written as

$$A_1 + A_2 = \sqrt{(A_1 + A_2)^2} = \sqrt{A_1^2 + A_2^2 + 2\,A_1\,A_2}. \tag{B.12}$$

The comparison of Eqs. (B.11, B.12) shows that the relation $A_f \leqslant A_{\|}$ definitely holds if the following equation is satisfied:

$$\pi^2\,T_{1,2} \geqslant 2\,A_1\,A_2. \tag{B.13}$$

A way to prove the inequality above is to express the state vector variances and co-variances as functions of radar measurement accuracies in range (σ_R) and azimuth (σ_ϑ).

$$\sigma_x^2 = \sigma_R^2 \cos^2\vartheta + R^2\sigma_\vartheta^2 \sin^2\vartheta,$$

$$\sigma_y^2 = \sigma_R^2 \sin^2\vartheta + R^2\sigma_\vartheta^2 \cos^2\vartheta,$$

$$\sigma_{xy} = \frac{\sigma_R^2}{2}\sin 2\vartheta - \frac{R^2}{2}\sigma_\vartheta^2 \sin 2\vartheta. \tag{B.14}$$

The two radars S_1 and S_2 are supposed to be identical, so they are characterized by the same values of accuracy, both in range and azimuth. However, they are generally non co-located sensors, and this results in different pairs of coordinates, (R_1, ϑ_1) and (R_2, ϑ_2). Thus, we obtain

$$\sigma_{x,1}^2 = \sigma_R^2 \cos^2\vartheta_1 + R_1^2\sigma_\vartheta^2 \sin^2\vartheta_1,$$

$$\sigma_{y,1}^2 = \sigma_R^2 \sin^2\vartheta_1 + R_1^2\sigma_\vartheta^2 \cos^2\vartheta_1,$$

$$\sigma_{xy,1} = \frac{\sigma_R^2}{2}\sin 2\vartheta_1 - \frac{R_1^2}{2}\sigma_\vartheta^2 \sin 2\vartheta_1, \tag{B.15}$$

$$\sigma_{x,2}^2 = \sigma_R^2 \cos^2\vartheta_2 + R_2^2\sigma_\vartheta^2 \sin^2\vartheta_2,$$

$$\sigma_{y,2}^2 = \sigma_R^2 \sin^2\vartheta_2 + R_2^2\sigma_\vartheta^2 \cos^2\vartheta_2,$$

$$\sigma_{xy,2} = \frac{\sigma_R^2}{2}\sin 2\vartheta_2 - \frac{R_2^2}{2}\sigma_\vartheta^2 \sin 2\vartheta_2. \tag{B.16}$$

By means of Eqs. (B.15, B.16), the first term of Eq. (B.13) becomes:

$$\begin{aligned}\pi^2\,T_{1,2} &= \pi^2\,(\sigma_{x,1}^2\,\sigma_{y,2}^2 + \sigma_{x,2}^2\,\sigma_{y,1}^2 - 2\,\sigma_{xy,1}\,\sigma_{xy,2}) \\ &= \pi^2\left\{[\sigma_R^4 + \sigma_\vartheta^4 R_1^2 R_2^2 - \sigma_R^2\,\sigma_\vartheta^2(R_1^2 + R_2^2)]\sin^2(\vartheta_2 - \vartheta_1) + \sigma_R^2\,\sigma_\vartheta^2(R_1^2 + R_2^2)\right\}.\end{aligned} \tag{B.17}$$

The second term of Eq. (B.13) is instead

$$2\,A_1\,A_2 = 2\pi^2 R_1 R_2 \sigma_R^2 \sigma_\vartheta^2. \tag{B.18}$$

Eq. (B.13) finally becomes

$$\begin{aligned}&[\sigma_R^4 + \sigma_\vartheta^4 R_1^2 R_2^2 - \sigma_R^2\sigma_\vartheta^2(R_1^2 + R_2^2)] \\ &\quad \sin^2(\vartheta_2 - \vartheta_1) + \sigma_R^2\sigma_\vartheta^2(R_1^2 + R_2^2) \geqslant 2R_1R_2\sigma_R^2\sigma_\vartheta^2.\end{aligned} \tag{B.19}$$

After some manipulation, we obtain

$$[\sigma_R^4 + \sigma_\vartheta^4 R_1^2 R_2^2 - \sigma_R^2\sigma_\vartheta^2(R_1^2 + R_2^2)] \quad \sin^2(\vartheta_2 - \vartheta_1) + \sigma_R^2\sigma_\vartheta^2(R_1 - R_2)^2 \geqslant 0. \tag{B.20}$$

In order to prove that the relationship above always holds, whatever are the values of $R_1, R_2, \vartheta_1, \vartheta_2$, we should consider the sign of the expression in Eq. (B.20) among square brackets. If it is positive, then Eq. (B.20) is always proved, regardless the value of $\sin^2(\vartheta_2 - \vartheta_1)$. If instead the expression among square brackets is negative, then the minimum value which can be assumed by the global expression is obtained when the expression among square brackets is multiplied by 1. In other words, if $\sin^2(\vartheta_2 - \vartheta_1) = 1$, Eq. (B.20) becomes

$$\sigma_R^4 + \sigma_\vartheta^4 R_1^2 R_2^2 - \sigma_R^2 \sigma_\vartheta^2 (R_1^2 + R_2^2) + \sigma_R^2 \sigma_\vartheta^2 (R_1 - R_2)^2 \geqslant 0. \tag{B.21}$$

After simplification, we obtain

$$(\sigma_R^2 - \sigma_\vartheta^2 R_1 R_2)^2 \geqslant 0, \tag{B.22}$$

which is always true.

Eq. (B.13) has been proved by means of Eq. (B.22), so ensuring that Eq. (B.10) is always satisfied. In other words, the (x, y) estimate obtained by using two separate radars and fusing their tracks is more accurate than the estimate that would be obtained by applying the rule for in-parallel resistances ($A_f \leqslant A_\parallel$).

Two particular configurations make A_f and $A_\parallel$ coincide:

(1) Radars S_1 and S_2 are co-located and their state vector estimates are characterized by identical covariance matrices ($\mathbf{P}_1 \equiv \mathbf{P}_2$). Under this hypothesis, uncertainty areas are equal as well ($A_1 = A_2 = A$) and the equivalent area is given by

$$A_f = \frac{A}{2}. \tag{B.23}$$

The same rule applies for identical resistances, whose value is halved when they are connected in parallel.

(2) Covariance matrices $\mathbf{P}_1$ and $\mathbf{P}_2$ are both diagonal, i.e. the two variables x and y are uncorrelated. Moreover, they are supposed to be characterized by the same standard deviation. These hypotheses can be represented as follows:

$$\sigma_{xy,1} = \sigma_{xy,2} = 0,$$

$$\sigma_{x,1} = \sigma_{y,1} = \sigma_1,$$

$$\sigma_{x,2} = \sigma_{y,2} = \sigma_2. \tag{B.24}$$

According to Eq. (B.24), we obtain

$$A_1 = \pi \sqrt{\sigma_{x,1}^2 \sigma_{y,1}^2 - \sigma_{xy,1}^2} = \pi \sigma_1^2,$$

$$A_2 = \pi \sqrt{\sigma_{x,2}^2 \sigma_{y,2}^2 - \sigma_{xy,2}^2} = \pi \sigma_2^2,$$

$$\pi^2 T_{1,2} = 2\pi^2 \sigma_1^2 \sigma_2^2 = 2 A_1 A_2. \tag{B.25}$$

The track fusion uncertainty area is finally given by

$$A_f = \frac{A_1 A_2}{A_1 + A_2} \equiv A_\parallel. \tag{B.26}$$

Physical considerations: Radar measurement accuracies σ_ρ and σ_ϑ can be both expressed as functions of the signal-to-noise ratio (SNR)

$$\sigma_\rho = \frac{\Delta R}{\sqrt{\mathrm{SNR}}},$$

$$\sigma_\vartheta = \frac{\Delta \vartheta}{\sqrt{\mathrm{SNR}}}, \tag{B.27}$$

where ΔR is the range resolution and $\Delta\vartheta$ is the -3 dB azimuth bandwidth.

Two radars S_1 and S_2 can be considered co-located either if they "collapse" into an equivalent radar having the same geometrical area and transmitting double power, either if they are connected back to back, so doubling the measurement data rate. In the former case, the SNR doubles as a consequence of the double transmitted power, in the latter case the equivalent SNR doubles as well, due to the double number of measurements (we assume there are no integration losses). Whatever the configuration, both standard deviations in (B.27) are reduced by a factor $\sqrt{2}$. Therefore, the state vector variances and co-variances in (B.14) become

$$\sigma_x^2 = \frac{\sigma_R^2}{2}\cos^2\vartheta + R^2\frac{\sigma_\vartheta^2}{2}\sin^2\vartheta,$$

$$\sigma_y^2 = \frac{\sigma_R^2}{2}\sin^2\vartheta + R^2\frac{\sigma_\vartheta^2}{2}\cos^2\vartheta,$$

$$\sigma_{xy} = \frac{\sigma_R^2}{4}\sin 2\vartheta - \frac{R^2}{4}\sigma_\vartheta^2 \sin 2\vartheta. \tag{B.28}$$

From (B.28), it can be easily computed that the uncertainty area halves, as previously demonstrated.

A geometrical and more intuitive explanation can also be given. Two co-located radars, tracking the same target, are characterized by identical uncertainty ellipsoids. The ellipsoid resulting from track-to-track fusion can be thought of as the envelope of a certain star of straight lines centered around the target. Along each straight line, the accuracy of the fused track is obtained according to the rule that applies to in-parallel resistances. Therefore, the extension of the fused track uncertainty ellipsoid along that straight line will be even shorter than the smaller of the axes of each ellipsoid. For the 2D case, the uncertainty ellipses associated to the tracks of co-located radars and to the fused track are depicted in Fig. B.1.

The same explanation applies to non co-located radars. Also in this case, the resulting ellipsoid can be constructed line by line, via the rule of in-parallel resistances, applied to 1D random variables; again, the lines pertain to the star with center on the target. A particular configuration analyzed in this section ($\mathbf{P}_1 = \sigma_1 \cdot \mathbf{I}, \mathbf{P}_2 = \sigma_2 \cdot \mathbf{I}$) corresponds to two uncertainty ellipsoids with null eccentricity, so degenerating into spheres. The resulting fused ellipsoid degenerates into a sphere, as well, and the gain of track-to-track fusion reduces to its upper bound, i.e. the value corresponding to the case of co-located radars ($\frac{1}{2}$ for 2D case). For a graphical example, refer to Fig. 5.

Appendix C

In this appendix it is proven that the inequality $V_f \leqslant V_\parallel$ holds also in the case when more than two radar sensors are considered. Let $S_1, S_2, \ldots, S_k$ be the k radar sensors considered, $k \geqslant 2$. Denote by $E_i = \{\mathbf{s}^{\mathrm{T}}\mathbf{P}_i^{-1}\mathbf{s} \leqslant r^2\}$ the ellipsoid of uncertainty associated to the target track estimated by the sensor S_i, where $\mathbf{s}$ represents the n-dimensional target state vector and $\mathbf{P}_i$ is an $n \times n$ positive definite matrix representing the

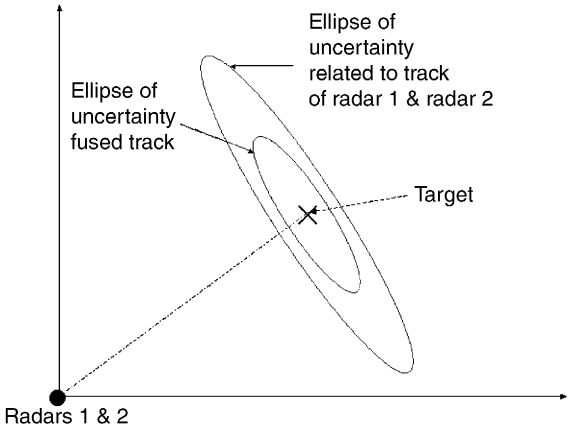

Fig. B.1. Uncertainty ellipses for co-located radars.

covariance matrix of the track. The volume V_f of the equivalent ellipsoid is given by

$$V_f = r^n c(n) = \frac{1}{\sqrt{\det(\mathbf{P}_f^{-1})}},$$

$$\mathbf{P}_f^{-1} = \mathbf{P}_1^{-1} + \mathbf{P}_2^{-1} + \cdots + \mathbf{P}_k^{-1}, \tag{C.1}$$

while the volume $V_{\parallel}$ obtained applying the rule of parallel resistances to the volumes $V_1, V_2, \ldots, V_k$ of the ellipsoids $E_1, E_2, \ldots, E_k$ is given by

$$V_{\parallel} = \frac{V_1 V_2 \cdots V_k}{V_2 V_3 \cdots V_k + V_1 V_3 \cdots V_k + \cdots + V_1 V_2 \cdots V_{k-1}},$$

$$V_i = r^n c(n) \frac{1}{\sqrt{\det(\mathbf{P}_i^{-1})}}. \tag{C.2}$$

The proof that the inequality $V_f \leqslant V_{\parallel}$ holds is based upon the following lemma.

Lemma 5. *Let* $\mathbf{A}_1, \mathbf{A}_2, \ldots, \mathbf{A}_k$, $k \geqslant 2$, *be* $n \times n$ *positive definite matrices*, $n = 1$. *Set an integer* $m = n$, *then it is true that*

$$[\det(\mathbf{A}_1 + \mathbf{A}_2 + \cdots + \mathbf{A}_k)]^{1/m} \geqslant [\det(\mathbf{A}_1)]^{1/m} + [\det(\mathbf{A}_2)]^{1/m} + \cdots + [\det(\mathbf{A}_k)]^{1/m}. \tag{C.3}$$

Proof. We proceed by induction on the number i of matrices considered.

Basic step: $i = 2$. It reduces to Corollary 2 proved in Appendix A.

Inductive step: $i + 1$. It is well known that the sum of two $n \times n$ positive definite matrices is an $n \times n$ positive definite matrix [12]. Setting $A = \mathbf{A}_1 + \mathbf{A}_2 + \cdots + \mathbf{A}_i$ and applying Corollary 2 we have

$$[\det(\mathbf{A} + \mathbf{A}_{i+1})]^{1/m} \geqslant [\det(\mathbf{A})]^{1/m} + [\det(\mathbf{A}_{i+1})]^{1/m}. \tag{C.4}$$

By inductive hypothesis we can state that

$$[\det(\mathbf{A})]^{\frac{1}{m}} \geqslant [\det(\mathbf{A}_1)]^{1/m} + [\det(\mathbf{A}_2)]^{1/m} + \cdots + [\det(\mathbf{A}_i)]^{1/m}. \tag{C.5}$$

Combining the inequalities (C.4) and (C.5) it follows immediately that:

$$[\det(\mathbf{A}+\mathbf{A}_{i+1})]^{1/m} \geqslant [\det(\mathbf{A}_1)]^{1/m} + [\det(\mathbf{A}_2)]^{1/m} + \cdots + [\det(\mathbf{A}_{i+1})]^{1/m}. \tag{C.6}$$

Since $\mathbf{A} = \mathbf{A}_1 + \mathbf{A}_2 + \cdots + \mathbf{A}_i$ by definition, the inequality (C.6) can be rewritten as

$$[\det(\mathbf{A}_1 + \mathbf{A}_2 + \cdots + \mathbf{A}_{i+1})]^{1/m} \geqslant [\det(\mathbf{A}_1)]^{1/m} + [\det(\mathbf{A}_2)]^{1/m} + \cdots + [\det(\mathbf{A}_{i+1})]^{1/m}, \tag{C.7}$$

which proves the inductive step. □

We are now ready to prove the main result of this appendix which is stated in the following form.

Theorem 6. *$V_f \leqslant V_\parallel$, where V_f and $V_\parallel$ have been defined, respectively, in* (C.1) *and* (C.2).

Proof. Using the expressions for V_f and $V_\parallel$ defined in (C.1) and (C.2) and reminding the basic result in matrix theory stating that $\det(\mathbf{AB}) = \det(\mathbf{A})\det(\mathbf{B})$ [12] we can write the inequality $V_f \leqslant V_\parallel$ as follows:

$$r^n c(n) \frac{1}{\sqrt{\det(\mathbf{P}_f^{-1})}} \leqslant \frac{[r^n c(n)]^k \left(\dfrac{1}{\sqrt{\det(\mathbf{P}_1^{-1}\mathbf{P}_2^{-1}\cdots\mathbf{P}_k^{-1})}} \right)}{[r^n c(n)]^{k-1} \left(\dfrac{1}{\sqrt{\det(\mathbf{P}_2^{-1}\mathbf{P}_3^{-1}\cdots\mathbf{P}_k^{-1})}} + \cdots + \dfrac{1}{\sqrt{\det(\mathbf{P}_1^{-1}\mathbf{P}_2^{-1}\cdots\mathbf{P}_{k-1}^{-1})}} \right)}, \tag{C.8}$$

which is true if and only if

$$r^n c(n) \frac{1}{\sqrt{\det(\mathbf{P}_f^{-1})}} \leqslant \frac{[r^n c(n)] \left(\dfrac{1}{\sqrt{\det(\mathbf{P}_1^{-1}\mathbf{P}_2^{-1}\cdots\mathbf{P}_k^{-1})}} \right)}{\left(\dfrac{\sqrt{\det(\mathbf{P}_1^{-1})} + \sqrt{\det(\mathbf{P}_2^{-1})} + \cdots + \sqrt{\det(\mathbf{P}_k^{-1})}}{\sqrt{\det(\mathbf{P}_1^{-1}\mathbf{P}_2^{-1}\mathbf{P}_3^{-1}\cdots\mathbf{P}_k^{-1})}} \right)}, \tag{C.9}$$

which is true if and only if

$$\sqrt{\det(\mathbf{P}_f^{-1})} \geqslant \sqrt{\det(\mathbf{P}_1^{-1})} + \sqrt{\det(\mathbf{P}_2^{-1})} + \cdots + \sqrt{\det(\mathbf{P}_k^{-1})}. \tag{C.10}$$

The inequality (C.10) is guaranteed to be true by the Lemma 5. This ends the proof of the theorem. □

Appendix D

Fact 1: The relationship between fused track and single track for co-located and non co-located radars.

Hypothesis: Let $E_1 = \{\mathbf{s}^T\mathbf{P}_1^{-1}\mathbf{s} \leqslant r^2\}$ and $E_2 = \{\mathbf{s}^T\mathbf{P}_2^{-1}\mathbf{s} \leqslant r^2\}, \ldots, E_k = \{\mathbf{s}^T\mathbf{P}_k^{-1}\mathbf{s} \leqslant r^2\}$ be the n-dimensional uncertainty ellipsoids associated to k radars. Let $\mathbf{P}_f^{-1} = \mathbf{P}_1^{-1} + \mathbf{P}_2^{-1} + \cdots + \mathbf{P}_k^{-1}$ and assume without loss of generality that E_1 has the maximum volume denoted by V_1.

Thesis: $\dfrac{V_f}{V_1} \leqslant \dfrac{1}{k}$.

Proof.

$$\frac{V_f}{V_1}=\frac{\sqrt{\det(\mathbf{P}_1^{-1})}}{\sqrt{\det(\mathbf{P}_f^{-1})}}=\frac{\sqrt{\det(\mathbf{P}_1^{-1})}}{\sqrt{\det(\mathbf{P}_1^{-1}+\mathbf{P}_2^{-1}+\cdots+\mathbf{P}_k^{-1})}}. \tag{D.1}$$

Applying Lemma 5 (which is reported in Appendix C) with $m=3$ we have that

$$\frac{\sqrt{\det(\mathbf{P}_1^{-1})}}{\sqrt{\det(\mathbf{P}_1^{-1}+\mathbf{P}_2^{-1}+\cdots+\mathbf{P}_k^{-1})}} \leqslant \frac{\sqrt{\det(\mathbf{P}_1^{-1})}}{\sqrt{\det(\mathbf{P}_1^{-1})}+\sqrt{\det(\mathbf{P}_2^{-1})}+\cdots+\sqrt{\det(\mathbf{P}_k^{-1})}}. \tag{D.2}$$

Since the volume of the generic ellipsoid $E_i=\{\mathbf{s}^{\mathrm{T}}\mathbf{P}_i^{-1}\mathbf{s}\leqslant r^2\}$ is given by $V_i=r^n c(n)1/\sqrt{\det(P_i^{-1})}$ and E_1 has the maximum volume among all ellipsoids, it must hold that $\sqrt{\det(\mathbf{P}_1^{-1})}\leqslant\sqrt{\det(\mathbf{P}_i^{-1})}$ for every $i=1,2,\ldots,k$. This allows us to state

$$\frac{\sqrt{\det(\mathbf{P}_1^{-1})}}{\sqrt{\det(\mathbf{P}_1^{-1})}+\sqrt{\det(\mathbf{P}_2^{-1})}+\cdots+\sqrt{\det(\mathbf{P}_k^{-1})}}\leqslant\frac{\sqrt{\det(\mathbf{P}_1^{-1})}}{k\sqrt{\det(\mathbf{P}_1^{-1})}}\leqslant\frac{1}{k}. \qquad \square \tag{D.3}$$

Fact 2: Lower bound for V_f.

Hypothesis: Let $E_1=\{\mathbf{s}^{\mathrm{T}}\mathbf{P}_1^{-1}\mathbf{s}\leqslant r^2\}$ and $E_2=\{\mathbf{s}^{\mathrm{T}}\mathbf{P}_2^{-1}\mathbf{s}\leqslant r^2\},\ldots,\ E_k=\{\mathbf{s}^{\mathrm{T}}\mathbf{P}_k^{-1}\mathbf{s}\leqslant r^2\}$ be the n-dimensional uncertainty ellipsoids associated to k radars.

Let $\mathbf{P}^{-1}=\mathbf{P}_i^{-1}: E_i$ is the ellipsoid with the minimum value and set $\mathbf{P}_{\min}^{-1}=\mathbf{P}_f+\mathbf{P}-1$. Call $V_{\min}$ the volume of the ellipsoid associated to the matrix $\mathbf{P}_{\min}^{-1}$.

Thesis: $V_{\min}\leqslant V_f$.

Proof.

$$\frac{V_f}{V_{\min}}=\frac{\sqrt{\det(\mathbf{P}_{\min}^{-1})}}{\sqrt{\det(\mathbf{P}_f^{-1})}}=\frac{\sqrt{\det(\mathbf{P}_f^{-1}+\mathbf{P}^{-1})}}{\sqrt{\det(\mathbf{P}_f^{-1})}}. \tag{D.4}$$

Since $\mathbf{P}_f^{-1}$ and $\mathbf{P}^{-1}$ are both positive definite matrices, due to Eq. (A.5) that

$$\frac{\sqrt{\det(\mathbf{P}_f^{-1}+\mathbf{P}^{-1})}}{\sqrt{\det(\mathbf{P}_f^{-1})}}\geqslant\frac{\sqrt{\det(\mathbf{P}_f^{-1})}+\sqrt{\det(\mathbf{P}^{-1})}}{\sqrt{\det(\mathbf{P}_f^{-1})}}\geqslant 1. \tag{D.5}$$

Being $(V_f/V_{\min})\geqslant 1$ we have that $V_{\min}\leqslant V_f$ which is exactly our thesis. $\square$

References

[1] A. Farina, F.A. Studer, Radar Data Processing Techniques, vol. 2: Advanced Topics and Applications, Research Studies Press, Wiley, New York, 1986.
[2] Y. Bar-Shalom, T. Fortmann, Tracking and data association, Academic Press, New York, 1988.
[3] S.S. Blackman, Multiple Target-tracking with Radar Applications, Artech House, Norwood, MA, December 1986.

[4] A. Farina, Sensor netting for surveillance and use of related emerging technologies, Proceedings of the 1987 Rome AFCEA European Symposium, May 6–8, 1987, pp. 49–57.
[5] H. Chen, T. Kirubarajan, Y. Bar-Shalom, Performance limits of track-to-track fusion versus centralized estimation: theory and application, IEEE Trans. Aerospace Electron. Systems 39 (2) (April 2003) 386–398.
[6] K.C. Chang, T. Zhi, R.K. Saha, Performance evaluation of track fusion with information matrix filter, IEEE Trans. Aerospace Electron. Systems 38 (2) (April 2002) 455–465.
[7] S. Mori, W.H. Barker, C.Y. Chong, K.C. Chang, Track association and track fusion with non deterministic target dynamics, IEEE Trans. Aerospace Electron. Systems 38 (2) (April 2002) 659–668.
[8] Y. Bar-Shalom, L. Campo, The effect of the common process noise on the two-sensor fused-track covariance, IEEE Trans. Aerospace Electron. Systems AES-22 (6) (November 1986) 803–805.
[9] S. Kay, Fundamentals of statistical signal processing, Estimation theory, Prentice Hall Signal Processing Theory, Prentice-Hall, Upper Saddle River, NJ, USA, 1993.
[10] M.I. Skolnik, Introduction to Radar Systems, McGraw-Hill, New York, 2003.
[11] M. Grotschel, L. Lovasz, A. Schrijver, Geometric algorithms and combinatorial optimization, Springer, Berlin, 1993.
[12] R. Bhatia, Graduate Texts in Mathematics, Matrix Analysis, vol. 16, Springer, New York, 1997, p. 47.